Physica B 405 (2010) 2185–2188

Contents lists available at ScienceDirect

Physica B

journal homepage: www.elsevier.com/locate/physb

Relation between grazing incident X-ray diffraction and surface defects in silicon doped GaAs

J.A. Villada [a], S. Jiménez-Sandoval [a], M. López-López [b], L. Baños [c], M.E. Rodríguez-García [d,*]

[a] Centro de Investigación y de Estudios Avanzados del I.P.N., Unidad Querétaro, Libr. Norponiente No. 2000, Fracc. Real de Juriquilla, CP 76230 Querétaro, Qro., Mexico
[b] Departamento de Física, CINVESTAV-IPN, avenida IPN 2508, México DF, Mexico
[c] Instituto de Investigación en Materiales, UNAM, Ciudad Universitaria, México D.F., México
[d] Departamento de Nanotecnología, Centro de Física Aplicada y Tecnología Avanzada, Universidad Nacional Autónoma de México, Apartado Postal 1-1010 76000 Querétaro, Qro., México

ARTICLE INFO

Article history:
Received 23 November 2009
Received in revised form
29 January 2010
Accepted 1 February 2010

Keywords:
Silicon doped GaAs
Grazing incident X-ray diffraction
Oval defects

ABSTRACT

Grazing incident X-ray diffraction is used to study oval defects on the surface of silicon doped GaAs layers grown by means of molecular beam epitaxy. The amplitude of the (1 1 3) peak from the diffraction data is associated with the defect density obtained from scanning electron microscopy images. These images reveal two different kinds of defects for all samples. It was proven that variations in the silicon effusion cell temperature affect the defect density. By increasing the cell temperature the defect density increases.

1. Introduction

III–V semiconductor heterostructures, containing GaAs, are currently used in a large variety of microelectronic and optoelectronic devices such as high electron mobility transistors (HEMTs) [1], light emission diodes [2], and lasers [3]. Surface self-assembled quantum dots can be including as structures that provide novel properties for the design of new functional devices [4]. However, different kinds of defects and structures, like pits [5], hillocks [6], and oval defects [7–10] are typically formed on the GaAs surface when it is grown by molecular beam epitaxy (MBE). As a rule, all of them hinder the elaboration of abrupt heterojunctions. Therefore, a proper characterization of the origin of these defects is necessary in order to obtain reliable devices.

Size and density, defined as the number of defects per unit area, are the principal parameters used to characterize the aforementioned structures. Scanning electron microscopy (SEM) and atomic force microscopy (AFM) are usually employed to obtain both density and size of structures. Since these structures can be as small as a few nanometers and are distributed across the entire surface, it is necessary to take several images from the surface in order to acquire enough information that allows a valid statistical analysis. Therefore, the main drawback of this methodology is the large amount of time required to yield valuable data. This problem can be solved using a technique that can probe a large portion of the surface without losing information from individual defects.

Grazing incident X-ray diffraction (GIXRD) is the most common technique for this type of analyses in thin films because it can provide information about structures near to or on the surface. In GIXRD the stationary incident beam makes a very small angle with the sample (between 1° and 5°), which increases the path length of the X-ray beam through the film. Consequently, an increment in the diffracted intensity from the thin film is observed while, at the same time, a reduction in the diffracted intensity from the bulk or substrate is achieved. In addition, since the incident beam is almost parallel to the surface, GIXRD can provide information regarding surface structures.

Zhang et al. [11] and Kondrashkina et al. [12] have used GIXRD to study the distribution of InAs quantum dots on GaAs and defects in crystal surface layers, respectively. However, in both cases the information was obtained from the diffuse scattering of the diffraction data. As a result, the information may contain a considerable error in comparison to the information obtained from a well resolved peak.

In this paper we show experimentally that it is possible to use a well resolved GIXRD peak to obtain information of the epitaxially grown structures. The study was carried out on the so-called oval defects, one of the most common structures present in MBE grown semiconductor layers [7–8,13,14]. Seven samples of silicon (Si) doped GaAs were grown by MBE with different Si effusion cell temperatures, from 1120 to 1330 °C, in order to obtain layers with different dopant concentrations. SEM was used to study both the morphology and defect densities. GIXRD was

* Corresponding author.
E-mail address: marioga@fata.unam.mx (M.E. Rodríguez-García).

0921-4526/$ - see front matter © 2010 Elsevier B.V. All rights reserved.
doi:10.1016/j.physb.2010.02.003

employed to detect the existence of crystal structures close to the surface, and the peak intensity of the [1 1 3] direction was associated to the defect density obtained by SEM images. Moreover, we found that varying the temperature of the Si effusion cell, different concentrations of oval defects were obtained.

2. Material and methods

2.1. Sample description

Semi-insulator undoped GaAs (0 0 1) wafers from Atramet Inc., USA possessing a resistivity of $10^8\,\Omega$/cm; an etch pit density (EPD) less than $8\times10^3\,cm^{-2}$ polished on both sides, with a diameter of 50.8 mm and thickness of 400 μm (epi-ready) were used in this study as substrates to grow a set of seven Si-doped GaAs samples. The samples were grown in a Riber C21 molecular beam epitaxy (MBE) system. The temperature of the Si effusion cell was varied from 1120 to 1330 °C in order to obtain GaAs layers with different Si concentrations. Table 1 shows the temperature of the Si effusion cell employed in each sample. Parameters such as substrate temperature, gallium effusion cell temperature, and growth time remained constant. The temperature of the doping (Si) effusion cell was the only parameter that was varied.

2.2. SEM analysis

SEM images of the samples surface were obtained utilizing a Jeol JSM-6060 LV microscope employing 20 and 25 kV acceleration voltages. Owing to the fact that the size of defects is different for each sample, the amplification was adjusted to obtain images with sides measuring approximately ten times the size of the defect. The density of the defects was determined from the average density obtained from 40 different images per sample.

2.3. GIXRD

Grazing X-ray measurements were performed in a Siemens D500 diffractometer with a CuKα radiation, employing a grazing angle accessory, a secondary graphite monochromator, and a scintillation detector. The incoming angle was 1° and the penetration depth for this angle was approximately 7 nm.

3. Results

3.1. SEM

3.1.1. Morphologies

Fig. 1 shows two different defect morphologies found in the MBE Si-doped GaAs layers. The defect shown in Fig. 1(a) has an average size of 4 μm. In the SEM image it looks like two separate defects, but a closer inspection reveals that these two structures belong to one larger defect with hexagonal geometry. The image has been highlighted with a hexagon to facilitate viewing. In papers about defect classifications for MBE GaAs [15] there is no information related to the formation of this kind of defect.

Table 1
Si effusion cell temperature employed in the growth of the studied samples.

Sample	43	44	45	46	64	65	66	67
Si effusion cell temperature (°C)	1330	1300	1270	1240	1200	1180	1140	1120

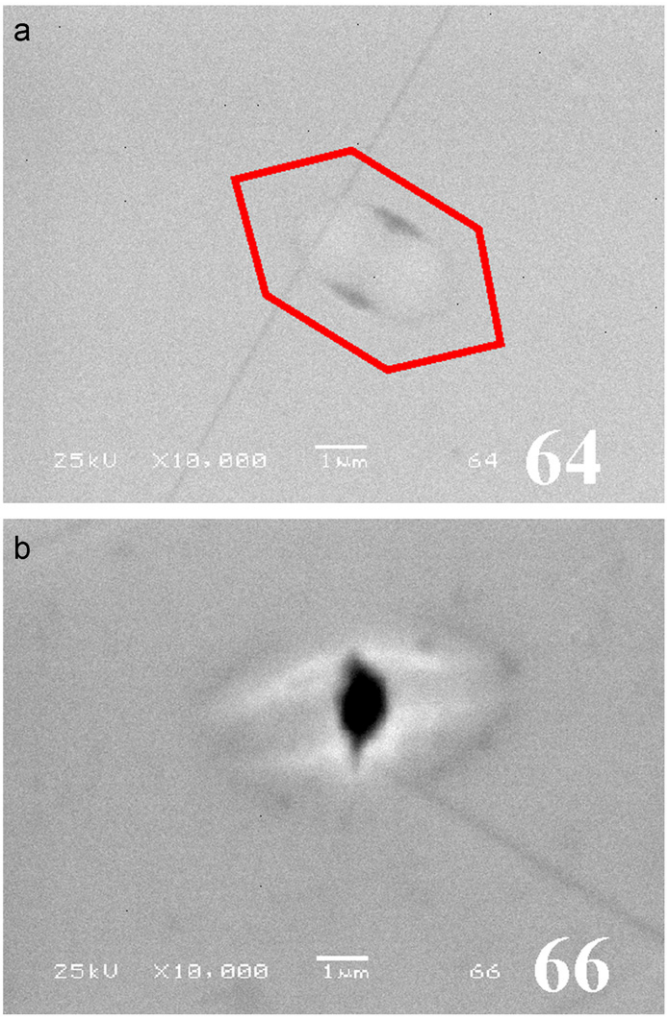

Fig. 1. SEM micrographs of two different kinds of defects as present in MBE GaAs layers.

A second kind of defect is shown in Fig. 1(b). This defect is similar to those presented by Fujiwara et al. [15] as defects "type β", but in the case of Si-doped GaAs, the average size is 3 μm.

An important feature of these defects is that they have a preferential orientation; this feature is shown in Fig. 2. The preferential orientation can be explained by the anisotropy of the diffusion coefficient of the adatoms on the substrate [16]. By using SEM images and taking into account the cleavage direction of the samples, it is possible to establish that the defects are aligned along the [1 1 0] direction. These defects always appear in pairs, and upon completion of a detailed inspection of Fig. 2, we found that these structures correspond to the defects illustrated in Fig. 1(a).

3.1.2. Defects density

Another important parameter related to defects is the density. Using SEM images it is possible to obtain the defect density as was aforementioned. Fig. 3 shows the defect density as a function of the Si effusion cell temperature. Defect density can be studied in two regions: for temperatures lower than 1200 °C and for temperatures higher than this value. In the first region, the defect density seems to be constant, while in the second region the defect density increases dramatically with the increase of cell temperature.

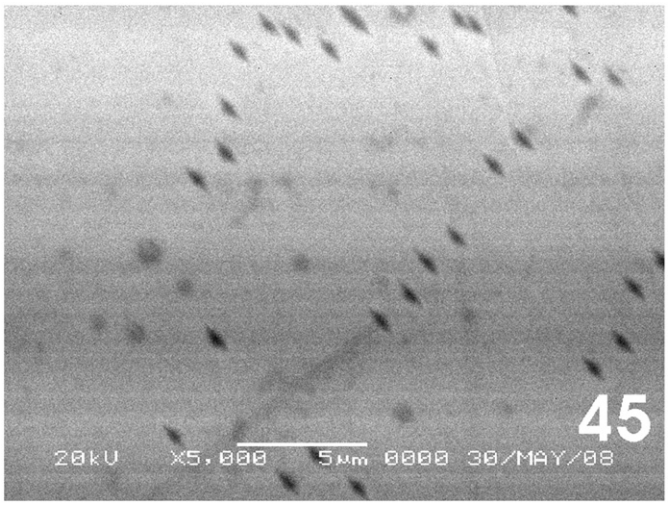

Fig. 2. SEM micrograph showing the preferential orientation of defects.

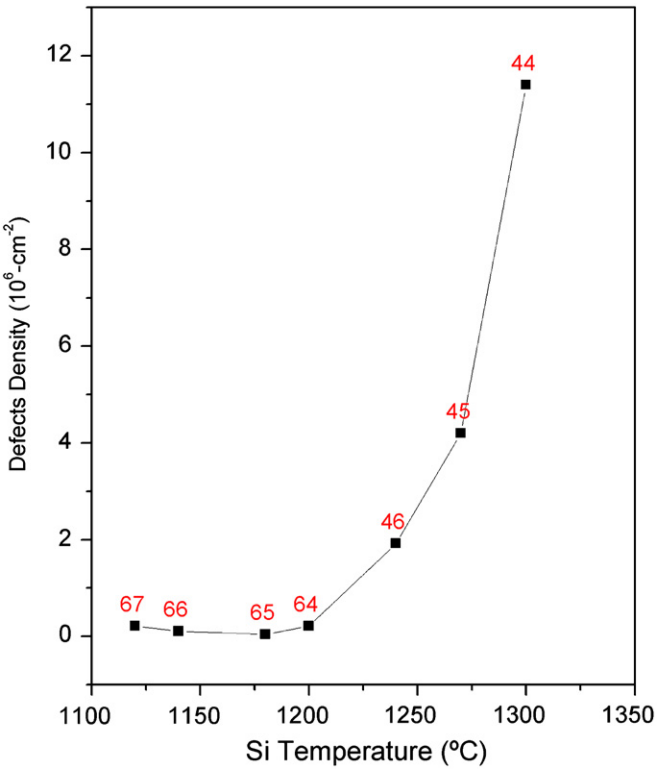

Fig. 3. Defects density as a function of the Si effusion cell temperature.

3.2. GIXRD study

Fig. 4 shows the GIXRD curves for all the samples studied. A highlight characteristic of this GIXRD curve is that the peak associated to the (1 1 3) direction is the only peak present, although the substrate has (0 0 1) orientation. The existence of this unique peak is a proof that the defects have a crystalline orientation. Otherwise, polycrystalline or amorphous defects could generate multi-peaks or broad bands, respectively.

It is known [17,18] that the (1 1 3) peak is observed in GIXRD because the angle between (0 0 1) and (1 1 3) planes (25.24°) is approximately equal to the Bragg angle for (1 1 3) diffraction (26.87°). In addition, under the angle of incidence of 1° with respect to the (0 0 1) oriented surface the incoming beam may take up the right angle for the (1 1 3) direction. The X-ray diffraction intensity for the (1 1 3) characteristic peak as a function of the Si effusion cell temperature is shown in Fig. 5. It is clear that for samples grown at temperatures higher than 1200 °C the intensity increases. Taking into account Figs. 4 and 5 it is evident that the (1 1 3) GIXRD intensity is associated to the defects density.

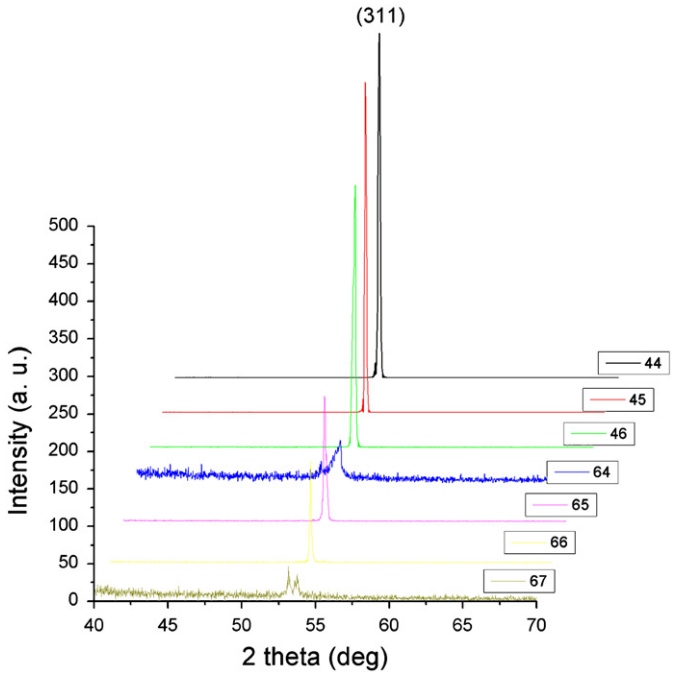

Fig. 4. Grazing X-ray diffraction curves for all samples.

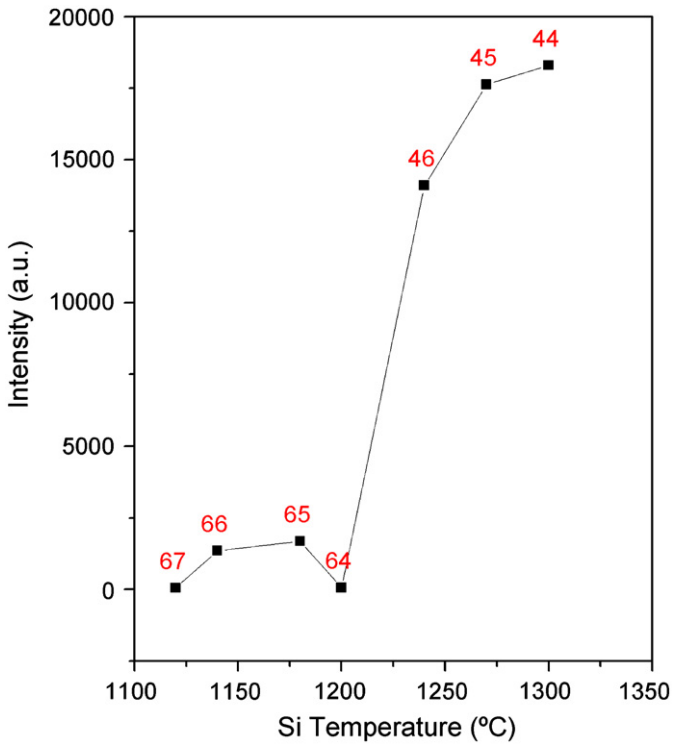

Fig. 5. Intensity of the (1 1 3) X-ray peak as a function of Si effusion cell temperature.

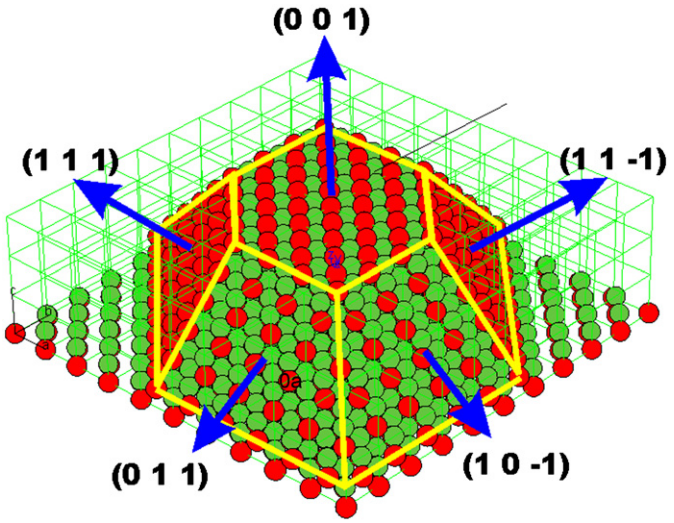

Fig. 6. Scheme of an oval defect on (0 0 1) surface.

It is necessary to have in mind that GIXRD is able to detect the crystalline structures close to or over the surface. Consequently, the relationship between the GIXRD intensity and the defects density can be explained by two factors as follows: first, the defects introduce disorder which helps to accommodate the right conditions for the (1 1 3) Bragg diffraction. If the defects density increases, this disorder increases as well. The disorder enhances the probability of taking the (1 1 3) direction, for this reason the GIXRD intensity follows the same behavior of the density. A second factor is that the defects are formed by planes arising from the surface with the same crystalline orientation of the layer. These planes can be easily detected by GIXRD. When the defect density of the layer increases, the X-ray beam can obtain more information regarding these planes and the GIXRD intensity increases. Fig. 6 shows a proposed structure of a defect formed by a (0 0 1) plane limited by a combination of (1 1 1) and (1 1 0) planes in the lateral facets. This structure reproduces the shape of the defect shown in Fig. 1(a). From Figs. 3 and 5 it is evident that the changes of the Si effusion cell temperature produce, not only different Si concentration, but also different defect densities in the MBE Si-doped GaAs layers.

4. Conclusions

It has been demonstrated that the temperature of the dopant effusion cell is associated with the formation of defects in the surface of MBE layers of GaAs. The defects were observed in the entire set of studied samples. However, their density was related to the temperature of the Si effusion cell. For samples grown with the Si cell at high temperatures ($T > 1250\,^{\circ}C$) the defect density is greater than in samples grown with the Si cell at lower temperatures, Fig. 3. In addition, these defects have a preferential alignment along the [1 1 0] direction on the surface.

The intensity of the (1 1 3) direction peak, obtained by means of grazing X-ray diffraction, can be related to the density of defects for each sample. If the defect density increases, the grazing X-ray diffraction intensity increases as well.

Acknowledgments

This work was partially supported by project no. PAPIIT IN120809 2009/11, Universidad Nacional Autónoma de México, CONACYT-México, and ICTDF. The authors would like to thank the technical assistance of Alicia Del Real, R. Fragoso, and E. Gomez. J.A. Villada would also like to personally thank CONACYT for the financial support for his Ph.D. studies.

The authors would like thank to Silvia C. Stroet of the Engineering Faculty at UAQ University, for her technical support in editing the English of this paper.

References

[1] W.C. Chang, T.C. Cheng, K.F. Yarn, J. Optoelectron. Adv. Mater. 8 (2006) 329.
[2] S.I. Tsintzos, P.G. Savvidis, G. Deligeorgis, Z. Hatzopoulos, N.T. Pelekanos, Appl. Phys. Lett. 94 (2009) 071109.
[3] A.V. Aluev, A.M. Morozyuk, M.Sh. Kobyakova, A.A. Chel'nyi, Quantum Electron. 31 (2001) 627.
[4] J.S. Rojas-Ramírez, A. Pulzara-Mora, E. Cruz-Hernandez, A. Perez-Centeno, M. Melendez-Lira, V.H. Mendez-Garcia, M. López-López, Physca E 32 (2006) 139.
[5] A. Pulzara-Mora, M. Meléndez-Lira, C. Falcony Guajardio, M. Lopez-Lopez, M.A. Vidal, S. Jiménez-Sandoval, M.A. Aguilar-Frutis, J. Vac. Sci. Technol. B 24 (2006) 1591.
[6] V.H. Mendez-Garcia, F.J. Ramirez-Arenas, A. Lastras-Martinez, E. Cruz-Hernandez, A. Pulzara-Mora, J.S. Rojas-Ramirez, M. Lopez-Lopez, Appl. Surf. Sci. 252 (2006) 5530.
[7] N.J. Kadhim, D. Mukhejee, Jour. Matt. Scienc.. Mater. Sci. Lett. 17 (1998) 595.
[8] K. Klima, M. Kaniewska, K. Regiñski, J. Kaniewski, Cryst. Res. Technol. 34 (1999) 683.
[9] J.M.E. Haverkort, M.P. Schuwer, M.R. Leys, J.H. Wolter, Semicond. Sci. Technol. 7 (1992) A59.
[10] H. Kawada, S. Shirayone, K. Takahashi, J. Crystal. Growth 128 (1993) 550.
[11] K. Zhang, J. Falta, Th. Schmidt, Ch. Heyn, G. Materlik, W. Hansel, Pure Appl. Chem. 72 (2000) 199.
[12] E.A. Kondrashkina, S.A. Stepanov, M. Schmidbauer, R. Opitz, R. Kohler, H. Rhan, J. Appl. Phys. 81 (1997) 175.
[13] H. Kakibayashi, F. Nagata, Y. Katayama, Jpn. J. Appl. Phys. 23 (1984) L846.
[14] Y. Suzuki, M. Seki, Y. Horikoshi, H. Okamoto, Jpn. J. Appl. Phys. Lett. 23 (1984) 164.
[15] K. Fujiwara, K. Kanamoto, Y.N. Ohta, Y. Tokuda, T. Nakayama, J. Crystal. Growth 80 (1987) 104.
[16] T. Nishinaga, J. Crystal. Growth 146 (1995) 326.
[17] E. Pinĕíeık, M. Jergel, M. Kucera, R.A.C.M.M. van Swaaij, J. Ivanco, R. Senderak, M. Zeman, J. Mullerova, M. Brunel, Appl. Surf. Sci. 166 (2000) 72.
[18] E. Pinĕík, M. Jergel, M. Kueèra, M. Brunel, Thin Solid Films 299 (1997) 136.